THE JOURNAL OF BIOLOGICAL CHEMISTRY VOL. 281, NO. 5, pp. 2945–2950, February 3, 2006

Transient IκB Kinase Activity Mediates Temporal NF-κB Dynamics in Response to a Wide Range of Tumor Necrosis Factor-α Doses*[S]

Received for publication, September 14, 2005, and in revised form, November 21, 2005 Published, JBC Papers in Press, December 1, 2005, DOI 10.1074/jbc.M510085200

Raymond Cheong[‡1], Adriel Bergmann[‡], Shannon L. Werner[§], Joshua Regal[§], Alexander Hoffmann[§], and Andre Levchenko[‡2]

From the [‡]Department of Biomedical Engineering, Johns Hopkins University, Baltimore, Maryland 21218 and the [§]Signaling Systems Laboratory, Department of Chemistry and Biochemistry, University of California, San Diego, San Diego, California 92093

Dynamic properties of signaling pathways control their behavior and function. We undertook an iterative computational and experimental investigation of the dynamic properties of tumor necrosis factor (TNF)α-mediated activation of the transcription factor NF-κB. Surprisingly, we found that the temporal profile of the NF-κB activity is invariant to the TNFα dose. We reverse engineered a computational model of the signaling pathway to identify mechanisms that impart this important response characteristic, thus predicting that the IKK activity profile must transiently peak at all TNFα doses to generate the observed NF-κB dynamics. Experimental confirmation of this prediction emphasizes the importance of mechanisms that rapidly down-regulate IKK following TNFα activation. A refined computational model further revealed signaling characteristics that ensure robust TNFα-mediated cell-cell communication over considerable distances, allowing for fidelity of cellular inflammatory responses in infected tissue.

The transcription factor NF-κB[3] is a key mediator of physiologic processes such as inflammation and adaptive immunity and has been implicated in numerous pathologic states such as cancer, rheumatoid arthritis, and sepsis (1). Consequently, understanding the mechanisms of NF-κB activation and regulation is of prime importance. One major activator of NF-κB is the potent inflammatory cytokine TNFα. TNFα binds to and trimerizes its receptor, TNFR1, which leads to a receptor-associated signalosome that activates the kinase IKK (2). IKK phosphorylates IκB proteins, which normally sequester NF-κB in the cytoplasm; phosphorylated IκBs are rapidly polyubiquitinated and proteasomally degraded, releasing free NF-κB, which translocates to the nucleus and modulates gene expression (2).

Detailed biochemical and genetic analyses over the past 25 years have helped elucidate the components that connect TNFα to NF-κB. However, relatively little is known about how these molecular players act together as a signaling system, whose complex dynamics control the time-variable activity of NF-κB and subsequent gene expression (3–6).

Recently, it has become apparent that analysis of the systems properties of complex biochemical pathways can benefit from an integrated approach combining systematic experimental perturbations with an associated computational analysis of molecular interactions (5, 7, 8, 10–13). This type of analysis applied to TNFα-induced NF-κB activity demonstrated that the α, β, and ε isoforms of IκB cooperate to produce a biphasic NF-κB response (5). Varying the duration of the TNFα stimulus had no effect on the duration of the initial response, thus ensuring expression of some NF-κB-regulated genes even in response to very short stimuli (5). This analysis, however, did not address the question of how other types of signaling inputs are processed.

In this study, we analyze in detail a different type of inputs, constant stimulations at different TNFα doses, and experimentally and computationally analyze the resulting pathway characteristics. Surprisingly, we found that both the duration and dose of TNFα stimulus have little effect on the duration of the initial NF-κB response and that NF-κB responds sensitively to an extremely wide range of TNFα concentrations. Analysis of a computational model of the pathway predicts that these signal transduction properties are crucially dependent on the transient nature of IKK activity. The experimental confirmation of this prediction underscores the importance of the mechanisms rapidly down-regulating IKK following its activation. Based on further model analysis, we suggest that the observed dynamic properties of IKK activity are well suited to offset limitations imposed by ligand diffusion, thereby ensuring robust TNFα-induced NF-κB activity in cells of infected tissues.

MATERIALS AND METHODS

Cell Lines and Tissue Culture—Immortalized 3T3 mouse embryonic fibroblasts (MEFs) were grown in Dulbecco's modified Eagle's medium with 10% bovine calf serum. Confluent, serum-starved (0.5% serum) cells were stimulated with murine TNFα (Roche Applied Science). In the experiments shown in Fig. 3*B*, cells were pretreated with 10 μg/ml cycloheximide (Sigma Chemicals) for 30 min prior to TNFα stimulation.

Electrophoretic Mobility Shift Assay—After TNFα stimulation, cells were washed with ice-cold phosphate-buffered saline + 1 mM EDTA, and were scraped and collected into a microcentrifuge tube and pelleted at 2000 × *g*. Cells (~10^6) were resuspended in 100 μl of CE buffer (10 mM HEPES-KOH (pH 7.9), 60 mM KCl, 1 mM EDTA, 0.5% Nonidet P-40, 1 mM dithiothreitol, 1 mM phenylmethylsulfonyl fluoride) and vortexed for lysis. Nuclei were pelleted at 4000 × *g*, resuspended in 30 μl of NE Buffer (250 mM Tris (pH 7.8), 60 mM KCl, 1 mM EDTA, 1 mM dithiothreitol, 1 mM phenylmethylsulfonyl fluoride), and lysed by three freeze-thaw cycles. Nuclear lysates were cleared by 14,000 × *g* centrifugation and the Bradford assay was used to determine protein concen-

* This work was supported in part by Grant GM072024-01 from the National Institutes of Health. The costs of publication of this article were defrayed in part by the payment of page charges. This article must therefore be hereby marked "*advertisement*" in accordance with 18 U.S.C. Section 1734 solely to indicate this fact.

[S] The on-line version of this article (available at http://www.jbc.org) contains supplemental information.

[1] Supported by the Medical Scientist Training Program at Johns Hopkins University.

[2] Supported by Grant GM69013-01/B270JA from the National Institutes of Health. To whom correspondence should be addressed: Dept. of Biomedical Engineering, Johns Hopkins University, 208C Clark Hall, 3400 N. Charles St., Baltimore, MD 21218. Tel.: 410-516-5584; Fax: 410-516-6240; E-mail: alev@jhu.edu.

[3] The abbreviations used are: NF-κB, nuclear factor-κB; IκB, Inhibitor of NF-κB; IKK, IκB kinase; TNFα, tumor necrosis factor α; MEF, murine embryonic fibroblast.

trations, which rarely varied by more than 30% from sample to sample. Protein concentrations were normalized by diluting the more concentrated samples in NE buffer. 2.5 μl of these samples was reacted at room temperature for 15 min with 0.01 pmol of ^{32}P-labeled 38-bp double-stranded oligonucleotide containing two consensus κB sites (GCTACAA**GGGACTTTCC**GCTG**GGGACTTTCC**AGGGAGG) in binding buffer (10 mM Tris-Cl (pH 7.5), 50 mM NaCl, 10% glycerol, 1% Nonidet P-40, 1 mM EDTA, 0.1 μg/μl poly(dIdC)), for a total reaction volume of 6 μl. Complexes were resolved on a nondenaturing 5% acrylamide (30:0.8) gel containing 5% glycerol and 1× TGE (24.8 mM Tris, 190 mM glycine, 1 mM EDTA) and were visualized using a PhosphorImager (Molecular Dynamics). The gel images were quantitated by drawing and integrating, for each lane, equally sized boxes around the NF-κB-specific DNA-protein complex, around the background above it, and around the unbound probe. The unbound probe was at >20-fold excess and was used as a loading control by taking the value of the signal minus the background then dividing by the unbound probe value. The resulting specific electrophoretic mobility shift assay signal was multiplied by 1000 or some constant to provide convenient arbitrary units.

IKK Kinase Assay—After TNFα stimulation, cytoplasmic extracts were isolated from cells as described above using 200 μl of IKK CE buffer (10 mM HEPES-KOH (pH 7.9), 250 mM NaCl, 1 mM EDTA, 0.5% Nonidet P-40, 0.2% Tween 20, 2 mM dithiothreitol, 1 mM phenylmethylsulfonyl fluoride, 20 mM β-glycerophosphate, 10 mM NaF, 0.1 mM Na_3VO_4) and were normalized via Bradford assay. Cytoplasmic extracts (100 μl) were incubated with 1 μg of IKKγ monoclonal antibody (BD Pharmingen) for 2 h at 4 °C and then with protein G-agarose-conjugated beads (Amersham Biosciences) for 1 h at 4 °C. After washing with IKK CE Buffer twice and kinase buffer (20 mM HEPES (pH 7.7), 100 mM NaCl, 10 mM $MgCl_2$, 2 mM dithiothreitol, 1 mM phenylmethylsulfonyl fluoride, 20 mM β-glycerophosphate, 10 mM NaF, 0.1 mM Na_3VO_4) once, the beads were incubated with 20 μl of kinase buffer containing 20 μM adenosine 5′-ATP, 10 μCi of [^{32}P]ATP, and 0.5 μg of bacterially expressed GST-IκBα (1–54) substrate at 30 °C for 30 min. The reaction was resolved by 10% SDS-PAGE and was visualized and quantitated by PhosphorImager. To normalize kinase activities, a portion of the SDS gel (175–50 kDa) was transferred to polyvinylidene difluoride (Amersham Biosciences) and probed for IKKα (Santa Cruz Biotechnologies) using standard immunoblotting techniques.

Canonical NF-κB Pathway Model—The basic model (ordinary differential equations, pre-equilibration initial conditions, and parameter values) has been published previously (5). The model was implemented in Cellerator 1.033 (14) and analyzed with Mathematica 4.2 and 5.0 (Wolfram Research). Some parameter values were modified according to Lipniacki *et al.* (15) (see section 1.3 of the supplemental information). For input reconstruction, we assumed an activation rate of the form shown in Equation 1 and a constant inactivation rate. We also assumed that changes in TNFα concentration uniformly and directly affect the activation rate function. The parameter space was exhaustively sampled within biochemically plausible ranges ($10^{-3} \le k_{init} \le 10^{-1}$ μM/min, $10^{0.25} \le k_{init}/k_{final} \le 10^{2}$, $5 \le \tau \le 30$ min, $10^{-2} \le k_{inact} \le 10^{1}$ min^{-1}), and results were filtered for resemblance to Fig. 1*B*, resulting in a unique set of parameters among those tested. See section 2 of the supplemental information for details.

TNFα Diffusion Simulation—Denoting C = [TNFα], then the spatiotemporal distribution $C(t,r)$ of TNFα, considering only the processes of diffusion and first-order degradation, is determined by the mass transfer equation $\partial C/\partial t = D\nabla^2 C - kC$. We assumed the diffusion constant $D = 2 \times 10^{-7}$ cm^2/s, in line with estimates for diffusible factors of similar size (16, 17). The parameter $k = 0.0275$ min^{-1}, corresponding to a half-life of 25 min, and represents loss of TNFα because of degradation and adherence to extracellular matrix proteins. TNFα secretion was modeled as a spherically symmetric flux of TNFα from a sphere of radius 10 μm, with the flux magnitude set so that the concentration at the source surface was ~10 ng/ml. With respect to time, TNFα secretion was modeled as a rectangular pulse of a 10-min duration. Finally, we imposed the boundary condition that $C \to 0$ as $r \to \infty$. The simulation was performed in Femlab 3.1 (Comsol, Burlington, MA). Simulations were run for different values of D, k, pulse length, and flux magnitude, which did not qualitatively affect any of the conclusions reported in the body of the paper. See section 3 of the supplemental information for extrapolation of the IKK response to arbitrary TNFα time courses.

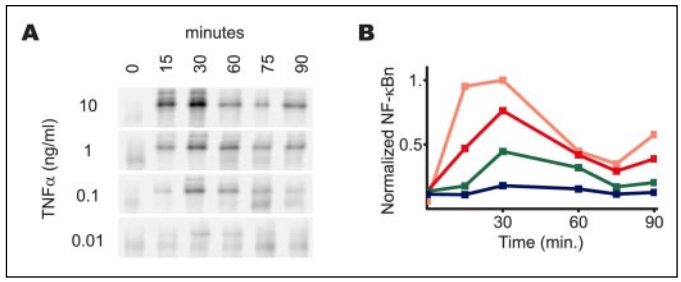

FIGURE 1. **NF-κB is sensitive to a wide range of TNFα concentrations.** *A*, dose response of cells to TNFα. Data shown are electrophoretic mobility shift assays of nuclear NF-κB from MEFs stimulated continuously with TNFα for the indicated time and dose. Results are representative of four other replicates. *B*, quantification of *A*, where 10, 1, 0.1, and 0.01 ng/ml TNFα are shown in *light red*, *red*, *green*, and *blue*, respectively.

RESULTS

NF-κB Is Sensitive to a Wide Range of TNFα Concentrations—To investigate the response of NF-κB to different TNFα doses, we exposed MEFs to TNFα over a concentration range spanning three orders of magnitude (0.01–10 ng/ml). NF-κB in these experiments was found to respond robustly and sensitively throughout this range, including the lowest dose of TNFα, as measured by electrophoretic mobility shift assay (Fig. 1*A*). This experiment, in which the duration of TNFα stimulation is held fixed (chronic) while altering the amplitude, complements our previous work in which the amplitude of TNFα was held fixed (10 ng/ml) while the duration was altered (5). Remarkably, in both cases, cells show a stereotypical response of an initial peak of NF-κB activity lasting 60–75 min (Fig. 1*B*). These results show that the NF-κB pathway is sensitive to a wide range of TNFα concentrations, which may help ensure a response to local TNFα signals in innate immune responses (see below).

Transient IKK Activity Generates Observed Dynamics in the Computational Model—To investigate the molecular basis underlying the robust dynamics of NF-κB activation, we attempted to recapitulate the dose response in our computational model of the NF-κB pathway. The model included detailed interactions between IKK, IκB, and NF-κB, and reflecting contemporary uncertainty about the mechanisms of IKK regulation (18), assumed an exponential decay curve for IKK during chronic TNFα stimulation. The model was previously validated for TNFα doses of 10 ng/ml, so to simulate lower TNFα concentrations we decreased the initial level of IKK. However, our simulation results did not adequately fit the measured responses as even a 10-fold reduction in IKK greatly delayed the onset of predicted NF-κB activity (Fig. 2*A*), suggesting that the model requires modification to recapitulate the experiment.

As a control, we first addressed whether the discrepancy between model prediction and experiment is because of a simple misestimation of rate constants described by the parameters in the model. Out of

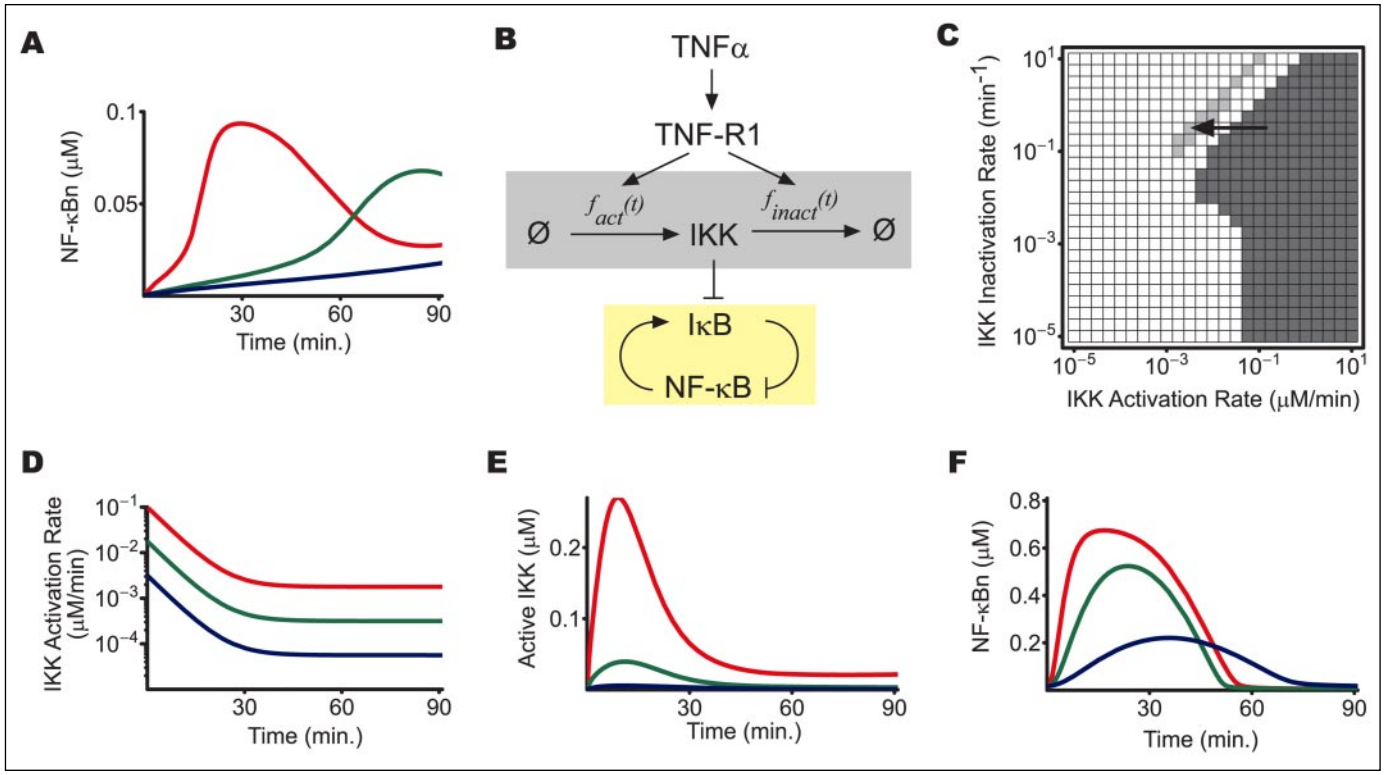

FIGURE 2. **Input constructed from the observed output rectifies the model.** *A*, model predictions do not agree with observed dynamics. The original model from Ref. 5 was run with initial IKK set to 0.10 (*red*), 0.02 (*green*), and 0.01 (*blue*) μM to simulate the effect of different TNFα doses. The predicted dynamics differ from the observed dynamics in Fig. 1. *B*, generalized model input scheme. A generator of IKK profiles was created (*gray box*) using arbitrary functions $f_{act}(t)$ and $f_{inact}(t)$ to represent the IKK activation and inactivation rates, respectively. The symbol "Ø" represents a source or sink for active IKK. The output of this profile generator feeds into the core model, influencing the behavior of the IκB-NF-κB negative feedback loop (*yellow box*). *C*, distribution of fits under a linear model of IKK regulation. The rate functions from *B* are assumed to be constant, and for each pair of rates tested the corresponding square is colored if the initial peak in NF-κB activity is high and timely (*dark gray*) or if the trough in NF-κB activity is low and timely (*light gray*). The regions do not overlap, showing that no pair of constant rates gives a complete fit to experiment and suggesting that a time-varying rate is needed (*arrow*). *D*, activation rate functions identified by exhaustive screening. Activation rates corresponding to high (*red*), medium (*green*), and low (*blue*) levels of TNFα are shown. *E*, the IKK and *F*, NF-κB activity time-courses predicted by the model using the functions in *D* and an inactivation rate of $k_{inact} = 0.1$ min^{-1}. Colors correspond to *D*.

10,000 parameter sets generated by random sampling within ± 2 orders of the nominal values, none fit the dose response while maintaining previously validated properties of the model (5). Sampling parameters in a way biased toward producing a fit, such as with evolutionary algorithms (19), also generated no fits. The results obtained by these naïve sampling methods were then confirmed by rational analysis of the model. Systematic dissection of how parameters influence key conserved features of the NF-κB temporal profile (peak timing and amplitude) revealed two independent effects, neither of which could be employed to reconcile the model and experiment without sacrificing previously validated properties of the model (see supplemental information, section 1). This rules out simple misestimation in parameter values as the source of discrepancy and suggests that the model should be extended to more fully describe the signaling pathway (20).

Because the model has successfully recapitulated several dynamic properties of the pathway (5), we surmised that the core model is essentially correct but that interactions with external components should be re-evaluated. One such component is the dynamic profile of IKK activity in response to TNFα stimulation, which serves as the input for the core model of the IκB-NF-κB signaling module (Fig. 2*B*). Thus we used the computational model to identify the temporal profiles of IKK activity that produce the observed NF-κB dynamics, essentially reverse engineering the input from the known output.

To screen for IKK profiles that could produce the NF-κB response, we created a generator of IKK temporal profiles and linked the generator to the model. This is shown schematically in Fig. 2*B*. Active IKK is generated through new protein synthesis or by activation from an inactive state according to some time-varying activation rate, then removed by protein degradation or inactivation according to some time-varying inactivation rate (Fig. 2*B*, *gray box*). One or both of these steps may be dependent on TNF receptor activation by TNFα. Additionally, IKK provides input into the core model (Fig. 2*B*, *yellow box*) by interacting with IκB, whose negative feedback to NF-κB is the central feature of the core model.

With the IKK profile generator written in this general form, our task is to identify activation and inactivation rate functions that produce the observed NF-κB dynamics. When both functions are temporally constant, no pair of rates can reproduce the response to high TNFα (Fig. 2*C*), suggesting that the regulation of IKK activity is nonlinear. To understand the nature of this nonlinearity, we examined the distribution of constant rates for which either the peak (Fig. 2*C*, *dark gray*) or the trough fit (Fig. 2*C*, *light gray*). Because all TNFα doses produce NF-κB temporal profiles that contain a peak between 15 and 45 min followed by a trough between 60 and 90 min (Fig. 1*B*), we concluded that the IKK activation rate may begin in the regime where the peak fits then decrease in time to the regime where the trough fits (as if to follow the *arrow* in Fig. 2*C*).

To test this possibility, we assumed a simple functional form (Equation 1) for an activation rate that decreases exponentially from a high initial value (k_{init}) to low final value (k_{final}) in about time τ, while holding the inactivation rate (k_{inact}) constant as seen here.

$$f_{act}(t) = (k_{init} - k_{final})(k_{init}/k_{final})^{-t/\tau} + k_{final} \quad \text{(Eq. 1)}$$

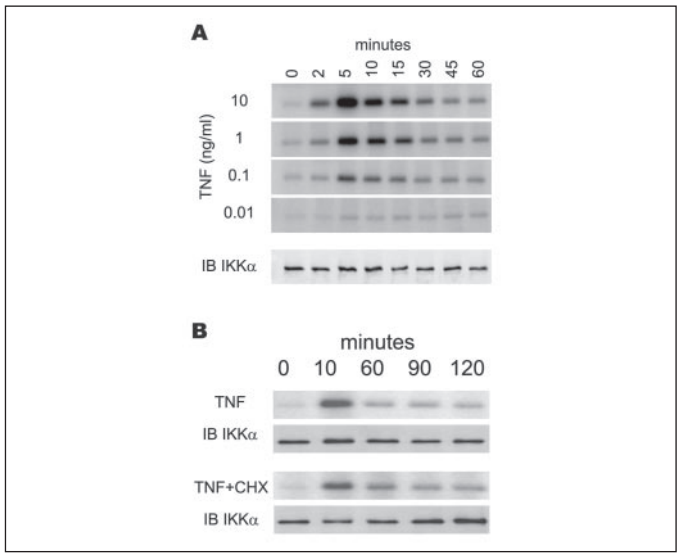

FIGURE 3. **Experiment validates prediction of transient IKK activity.** *A*, dose response of IKK activity. MEFs were stimulated with TNFα for the indicated time and dose, and kinase activity of immunoprecipitated IKK complex was measured against a GST-IκBα substrate. The *bottom panel* shows an example control for IKK complex immunoprecipitation efficiency. Timing of transient IKK activity matches the prediction in Fig. 2. *B*, IKK activity profile in MEFs following stimulation with 1 ng/ml TNFα for the indicated times in the presence or absence of 10 μg/ml cycloheximide. Immunoprecipitation controls are shown.

This functional form, combined with a simple method for representing different TNFα concentrations (see "Materials and Methods"), allowed us to fully specify the IKK profile in response to a range of TNFα with only four parameters. An exhaustive grid-based search of the parameter space (see supplemental information, section 2) uncovered exactly one parameter set out of 5615 tested that reproduces the response to different TNFα concentrations while maintaining previously validated properties of the model, suggesting that the observed output can only be produced by a very specific IKK activity profile. The activation rate functions thus identified (Fig. 2*D*) produce transient IKK activity at all TNFα doses (Fig. 2*E*) and result in NF-κB profiles (Fig. 2*F*) whose initial duration is fixed but whose amplitude varies with TNFα concentration, as desired. Thus, the model strongly suggests that the IKK activity profile has to be transient at all TNFα doses.

Predicted Transient IKK Activity Profile Is Verified Experimentally—The model-based reconstruction of IKK activity gives rise to an experimentally testable prediction: in response to a wide range of TNFα concentrations, IKK activity should peak at around 10 min and decrease over the next 20 min to a low level above basal activity (Fig. 2*E*). To further gauge the strength of this prediction, we chose other activation and inactivation rate functions to systematically test similarly shaped IKK profiles but with different peak timings and peak widths. The results showed that the specific profiles in Fig. 2*E* gave a near optimal fit with the experimentally measured NF-κB time courses (data not shown). Therefore, the dynamics of IKK activity are highly constrained. To validate this prediction, we measured the actual IKK activity in MEFs (Fig. 3*A*), revealing a very close agreement with the model predictions, especially in terms of the timing of the activation peak. Also, consistent with the idea that the IKK profile is highly constrained, IKK profiles display similar shape and timing when measured in multiple other cell types at 10 ng/ml TNFα or higher (21–26), although the significance of these IKK kinetics was not previously interpreted. The unexpected insight provided by our model, validated experimentally, is that a rapid decrease in IKK activity is required to explain the dependence of the amplitude, duration, and timing of the initial peak of NF-κB activity in response to a wide range of TNFα concentrations.

Given the requirement for fast IKK down-regulation in eliciting NF-κB activity in response to TNFα, we considered the question of what biochemical mechanisms could mediate it. The computational model does not strongly constrain the mechanism, because the activation and inactivation rate functions can be coordinately changed (equivalent to different biochemical mechanisms) without changing the overall IKK activity profile, resulting in the same NF-κB dynamics (data not shown). Instead, we considered this question in the context of known IKK inhibitors. One possible mediator of IKK down-regulation is A20, an inhibitor of RIP (27), which is transcriptionally up-regulated by NF-κB within 30 min (6), thus potentially forming a negative feedback loop. We explored whether, as previously suggested (15), A20 is essential for the control of dynamics of early IKK and NF-κB activation. However, IKK activity is down-regulated at 30 min following onset of stimulation even with very low concentrations of TNFα making it unlikely that feedback via A20 is solely responsible for regulating the dynamics of the IKK activity profile. Consistent with this, in cells exposed to cycloheximide, an inhibitor of new protein synthesis, IKK activity is still high at 10 min and low at 60 min (Fig. 3*B*). Furthermore, IKK activity in A20-deficient cells still shows a peak at around 10 min, although attenuation at later times is defective (24, 28). We also considered that if A20 negative feedback was solely responsible for early down-regulation of IKK, it would be difficult to infer IKK activity profiles from the NF-κB activity profile, as feedbacks generally preclude one-to-one input-output mapping. Although NF-κB-regulated IKK inhibitors like A20 may play a late role in IKK regulation, our results suggest that early IKK inhibition is likely not mediated by NF-κB up-regulation of A20 or similar feedback mechanism.

High Sensitivity of NF-κB to TNFα May Provide Robust Signaling at a Distance—Finally, we attempted to understand the dynamic properties of the pathway in a physiologic context. The primary physiologic function of TNFα is to mediate innate immune responses in response to infection (29). The effects of TNFα are local as enforced by multiple mechanisms. TNFα expression by pathogen-activated macrophages is brief and self-limited, because phagocytosis of pathogens rapidly removes the inciting stimulus, and prolonged exposure to TNFα can both lead to quick apoptosis of TNFα-secreting macrophages (30) and inappropriately induce systemic responses (31, 32). Several postinduction repression and autocrine inhibition mechanisms have been described for TNFα expression (33), and both TNFα mRNA and secreted protein have a short half-life (34–36). At the same time, the affinity of TNF to its receptors is similar to its affinity to extracellular matrix proteins (37) and the molecular mass of TNFα is high (51 kDa as active trimer), impeding diffusion and increasing buffering through nonspecific binding. All of these mechanisms serve to limit the effects of TNFα to a local tissue environment.

To model the local spread of TNFα in an infected tissue in a way consistent with the above, we considered the simple scenario in which a TNFα-secreting cell (or cluster of cells) produces a transient pulse of TNFα, which then diffuses into the surroundings, where it is subject to degradation and buffering. The real tissue environment is intricate and probably involves the presence of additional cytokines and more complex spatiotemporal patterns of TNFα secretion, but these simplifying assumptions can be viewed as a limiting case designed to investigate whether weak TNFα signaling can still be effective. Our simulations show that in this scenario nearby cells would experience a pulse of TNFα whose duration and amplitude both decrease rapidly with distance (Fig. 4, *A* and *B*, supplemental movie S1). We then considered how

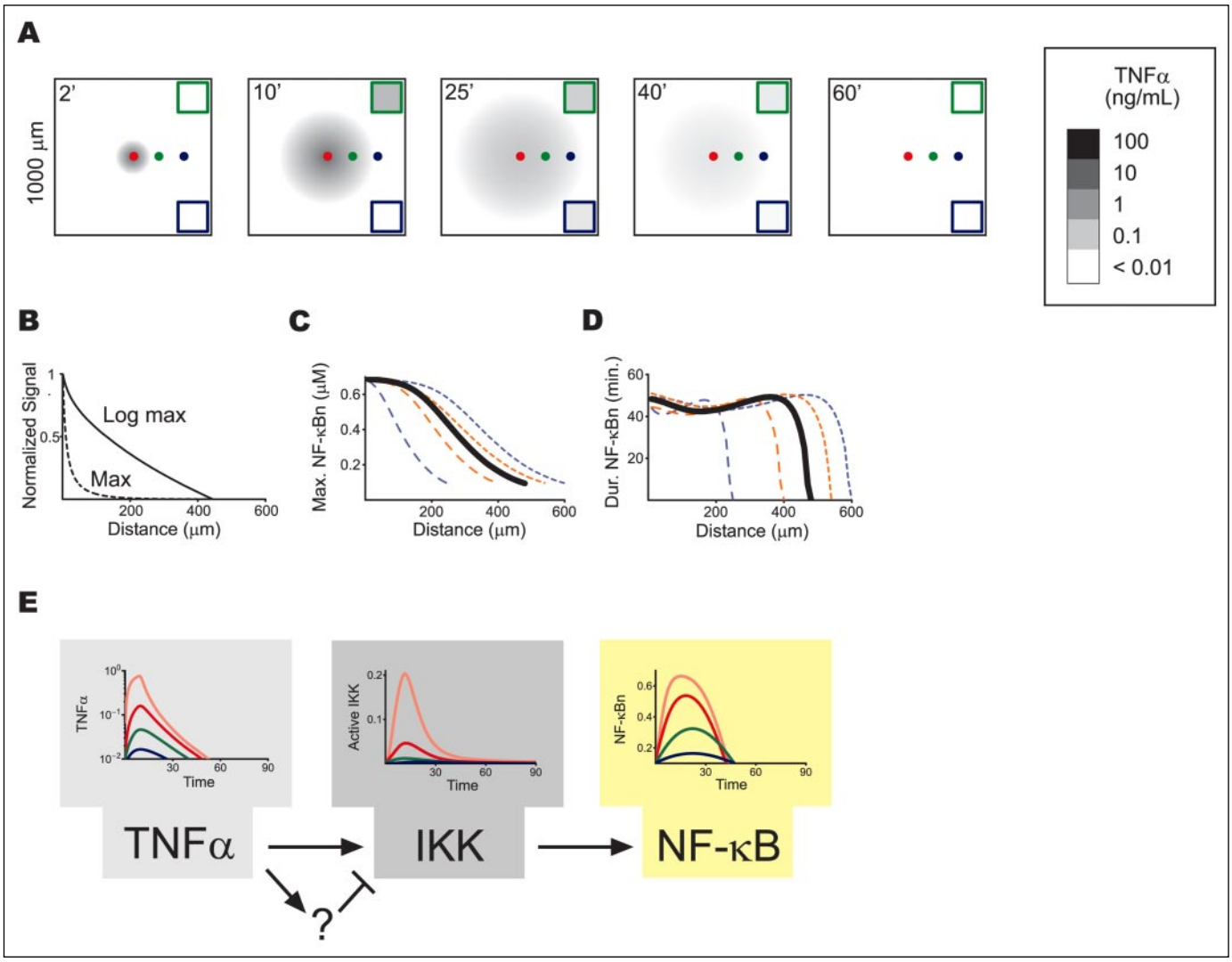

FIGURE 4. **NF-κB pathway dynamics may provide robust cell-cell signaling by TNFα diffusion.** *A*, simulation of diffusive spread of a pulse of TNFα in an infected tissue, causing nearby cells to experience pulses of TNFα of different amplitudes and durations. The *red circle* marks the TNFα source, and the *green* and *blue circles* mark points at which the local TNFα concentration is sampled at the indicated times, as shown in the *upper right* and *lower right* corners, respectively. The simulated region is a cube 1000 μm on each edge, and each panel represents a cross-section through the center of this space. See also supplemental movie 1. *B*, the maximum signal decays approximately exponentially with distance. Curves shown are maximum (*dashed*) and log maximum (*solid*) TNFα signal experienced because of diffusive spread, normalized to 0.01–10 ng/ml. *C* and *D*, simulated NF-κB response to TNFα time courses resulting from diffusive spread of a TNFα pulse. At nominal parameters (*solid black*), 6× flux (*dotted blue*), 0.2× flux (*dashed blue*), 20 min TNFα pulse (*dotted orange*), or 5 min TNFα pulse (*dashed orange*), the NF-κB response amplitude decays smoothly with distance, whereas duration of signaling (thresholded at 0.1 μM) is always 40–60 min. *E*, effect of distance on the TNFα, IKK, and NF-κB profiles. In each panel, simulated time courses at 100 (*light red*), 200 (*red*), 300 (*green*), and 400 (*blue*) μm from the source are shown, time-shifted for clarity. Due in part to fast IKK inhibition, distance-related changes in the amplitude and duration of the TNFα experienced (*light gray*) affect the amplitude but not temporal profile of IKK (*dark gray*) and NF-κB (*yellow*) activity.

target cells might respond to such local changes in TNFα concentration by coupling the TNFα diffusion simulation (Fig. 4*A*) to the NF-κB pathway model (Fig. 2*B*).

At various distances from the model TNFα source cell (*e.g.* a macrophage), we determined the local kinetic TNFα profiles due to diffusive spread and related them to the corresponding IKK activities (supplemental information, Section 3) and the resulting outputs of the NF-κB pathway. The simulations reveal that the NF-κB response amplitude (Fig. 4*C*) depends linearly on the distance from the TNFα source, whereas the duration of the response remains approximately constant (Fig. 4*D*). Furthermore, this qualitative behavior does not depend on the precise concentration or duration of the TNFα pulse (Fig. 4, *C* and *D*), nor on precise value of diffusivity or degradation rate/buffering strength (not shown). Rather, this signaling behavior is essentially because of the exponential drop of the maximum TNFα concentration with distance (Fig. 4*B*) coupled with logarithmic variation of the maximum NF-κB activity with TNFα input (Fig. 1*B*), and the remarkable independence of the duration of the initial NF-κB response on both the duration and the amplitude of the TNFα stimulus.

Importantly, the duration of NF-κB activity remains approximately constant even at distances (~500 μm) where the activity amplitude becomes negligible (Fig. 4, *C* and *D*). In comparison, the theoretical limit for cell-cell signaling has been estimated to be a few hundred microns (16). Thus, our results suggest that one function of the dynamic properties of the IKK/NF-κB pathway illuminated in this study is to provide a reliable and immediate response to TNFα even at limiting distances in infected tissue.

DISCUSSION

Here we undertook an iterative computational and experimental study of the dynamics of NF-κB in response to different TNFα doses. We present experimental data that show that NF-κB responds sensi-

tively to TNFα over a concentration range of three orders of magnitude. Interestingly, the duration of the initial response is constant with respect to TNFα dose, a dynamic property without an obvious mechanistic or teleologic explanation.

Computational modeling of NF-κB signaling helped suggest both the mechanistic basis and possible physiologic significance of the dynamic properties of the pathway. We found, by reconstructing the input into the IκB-NF-κB module, that one property mechanistically required for the observed NF-κB activity profiles is highly transient IKK activity with a peak at around 10 min following TNFα stimulation at different doses. Such reverse engineering may be useful in investigating other systems, but it is often difficult because of nonlinearities present in signaling systems and the large number of permissible input functions (38). We overcame these obstacles by starting with a simple linear case and using the results to guide the choice of nonlinear assumptions as well as by keeping the parameter space small to allow for exhaustive testing of all reasonable possibilities. Systematic perturbation of the revised model then indicated that the IKK activity was highly constrained by the observed output and this strong prediction was confirmed by kinase assays of IKKβ activity.

The molecular mechanism for fast inactivation of IKK remains mysterious. It is unlikely that postinduction attenuation of IKK activity is solely dependent on NF-κB-regulated IKK inhibitors like A20. Other IKK inhibitors like PP2Cβ, PP2A, CYLD, hTid-1, and Hsp70 might be involved (25, 39–44), or regulation of the conformational state of IKKβ via hyperautophosphorylation of its C terminus could lead to IKK inactivation (22). Importantly, the disruption of the C-terminal sites in IKKβ leads to persistently active IKK upon stimulation (22), suggesting inhibitory autophosphorylation as the major source of fast IKK down-regulation. High basal activity of IKK phosphorylation mutants prohibited us from easily testing this mechanism (22) but highlights the need for additional study into the mechanisms of IKK regulation.

The computational model also suggested how the characteristic NF-κB pathway dynamics might facilitate innate immunity in tissues during infection. TNFα may be secreted by a cell or a small cluster of cells (*e.g.* macrophages) thereby signaling to target cells located nearby. TNFα is a poor signaling agent because it is secreted briefly at low levels and diffuses slowly, but our results paint an intuitively appealing picture of why the local action of TNFα in innate immunity, acting through activation of NF-κB, can be both robust and efficient. TNFα can effectively activate NF-κB for prolonged periods in cells, possibly to ensure efficient triggering of gene transcription, even at near-limiting distances. The spatially graded nature of the response amplitude (Fig. 4*E*) also may ensure that cells respond commensurate with their distance from the source of danger (9), which could provide an economical result in which every responsive cell is neither excessively nor inadequately stimulated. These dynamic properties, in combination with information provided by other extracellular cues, could help prime and coordinate tissue responses to local infection. As such, IKK regulatory mechanisms may represent sensitive clinical targets in diseases with aberrant innate immune system activity.

REFERENCES

1. Cheong, R., and Levchenko, A. (2005) in *Encyclopedia of Molecular Cell Biology and Medicine* (Meyers, H. A., ed) Vol. 14, pp. 437–472, John Wiley & Sons, New York
2. Wajant, H., Pfizenmaier, K., and Scheurich, P. (2003) *Cell Death Differ.* **10,** 45–65
3. Barken, D., Wang, C. J., Kearns, J., Cheong, R., Hoffmann, A., and Levchenko, A. (2005) *Science* **308,** 52a
4. Hoffmann, A., Leung, T. H., and Baltimore, D. (2003) *EMBO J.* **22,** 5530–5539
5. Hoffmann, A., Levchenko, A., Scott, M. L., and Baltimore, D. (2002) *Science* **298,** 1241–1245
6. Zhou, A., Scoggin, S., Gaynor, R. B., and Williams, N. S. (2003) *Oncogene* **22,** 2054–2064
7. Bhalla, U. S., Ram, P. T., and Iyengar, R. (2002) *Science* **297,** 1018–1023
8. Ferrell, J. E., Jr., and Machleder, E. M. (1998) *Science* **280,** 895–898
9. Matzinger, P. (1998) *Semin. Immunol.* **10,** 399–415
10. Klein, D. E., Nappi, V. M., Reeves, G. T., Shvartsman, S. Y., and Lemmon, M. A. (2004) *Nature* **430,** 1040–1044
11. Ozbudak, E. M., Thattai, M., Lim, H. N., Shraiman, B. I., and Van Oudenaarden, A. (2004) *Nature* **427,** 737–740
12. Sasagawa, S., Ozaki, Y., Fujita, K., and Kuroda, S. (2005) *Nat. Cell. Biol.* **7,** 365–373
13. Swameye, I., Muller, T. G., Timmer, J., Sandra, O., and Klingmuller, U. (2003) *Proc. Natl. Acad. Sci. U. S. A.* **100,** 1028–1033
14. Shapiro, B. E., Levchenko, A., Meyerowitz, E. M., Wold, B. J., and Mjolsness, E. D. (2003) *Bioinformatics* **19,** 677–678
15. Lipniacki, T., Paszek, P., Brasier, A. R., Luxon, B., and Kimmel, M. (2004) *J. Theor. Biol.* **228,** 195–215
16. Francis, K., and Palsson, B. O. (1997) *Proc. Natl. Acad. Sci. U. S. A.* **94,** 12258–12262
17. Goodhill, G. J. (1997) *Eur. J. Neurosci.* **9,** 1414–1421
18. Ghosh, S., and Karin, M. (2002) *Cell* **109,** (suppl.) 81–96
19. Banzhaf, W. (1998) *Genetic Programming: an Introduction on the Automatic Evolution of Computer Programs and Its Applications*, Morgan Kaufmann, San Francisco, CA
20. von Dassow, G., Meir, E., Munro, E. M., and Odell, G. M. (2000) *Nature* **406,** 188–192
21. Aupperle, K. R., Bennett, B. L., Boyle, D. L., Tak, P. P., Manning, A. M., and Firestein, G. S. (1999) *J. Immunol.* **163,** 427–433
22. Delhase, M., Hayakawa, M., Chen, Y., and Karin, M. (1999) *Science* **284,** 309–313
23. DiDonato, J. A., Hayakawa, M., Rothwarf, D. M., Zandi, E., and Karin, M. (1997) *Nature* **388,** 548–554
24. Lee, E. G., Boone, D. L., Chai, S., Libby, S. L., Chien, M., Lodolce, J. P., and Ma, A. (2000) *Science* **289,** 2350–2354
25. Prajapati, S., Verma, U., Yamamoto, Y., Kwak, Y. T., and Gaynor, R. B. (2004) *J. Biol. Chem.* **279,** 1739–1746
26. Zandi, E., Rothwarf, D. M., Delhase, M., Hayakawa, M., and Karin, M. (1997) *Cell* **91,** 243–252
27. Wertz, I. E., O'Rourke, K. M., Zhou, H., Eby, M., Aravind, L., Seshagiri, S., Wu, P., Wiesmann, C., Baker, R., Boone, D. L., Ma, A., Koonin, E. V., and Dixit, V. M. (2004) *Nature* **430,** 694–699
28. Werner, S., Barken, D., and Hoffmann, A. (2005) *Science* **309,** 1857–1861
29. Tracey, K. J., and Cerami, A. (1992) *Proc. Soc. Exp. Biol. Med.* **200,** 233–239
30. Xaus, J., Comalada, M., Valledor, A. F., Lloberas, J., Lopez-Soriano, F., Argiles, J. M., Bogdan, C., and Celada, A. (2000) *Blood* **95,** 3823–3831
31. Blander, J. M., and Medzhitov, R. (2004) *Science* **304,** 1014–1018
32. Klein, R. D., Su, G. L., Schmidt, C., Aminlari, A., Steinstraesser, L., Alarcon, W. H., Zhang, H. Y., and Wang, S. C. (2000) *J. Surg. Res.* **94,** 159–166
33. Baer, M., Dillner, A., Schwartz, R. C., Sedon, C., Nedospasov, S., and Johnson, P. F. (1998) *Mol. Cell. Biol.* **18,** 5678–5689
34. Beutler, B. A., Milsark, I. W., and Cerami, A. (1985) *J. Immunol.* **135,** 3972–3977
35. Reeves, R., and Magnuson, N. S. (1990) *Prog. Nucleic Acids Res. Mol. Biol.* **38,** 241–282
36. Stoecklin, G., Lu, M., Rattenbacher, B., and Moroni, C. (2003) *Mol. Cell. Biol.* **23,** 3506–3515
37. Alon, R., Cahalon, L., Hershkoviz, R., Elbaz, D., Reizis, B., Wallach, D., Akiyama, S. K., Yamada, K. M., and Lider, O. (1994) *J. Immunol.* **152,** 1304–1313
38. Hartwell, L. H., Hopfield, J. J., Leibler, S., and Murray, A. W. (1999) *Nature* **402,** Suppl. 6761, 47–52
39. Brummelkamp, T. R., Nijman, S. M., Dirac, A. M., and Bernards, R. (2003) *Nature* **424,** 797–801
40. Cheng, H., Cenciarelli, C., Nelkin, G., Tsan, R., Fan, D., Cheng-Mayer, C., and Fidler, I. J. (2005) *Mol. Cell. Biol.* **25,** 44–59
41. Fu, D. X., Kuo, Y. L., Liu, B. Y., Jeang, K. T., and Giam, C. Z. (2003) *J. Biol. Chem.* **278,** 1487–1493
42. Kovalenko, A., Chable-Bessia, C., Cantarella, G., Israel, A., Wallach, D., and Courtois, G. (2003) *Nature* **424,** 801–805
43. Ran, R., Lu, A., Zhang, L., Tang, Y., Zhu, H., Xu, H., Feng, Y., Han, C., Zhou, G., Rigby, A. C., and Sharp, F. R. (2004) *Genes Dev.* **18,** 1466–1481
44. Trompouki, E., Hatzivassiliou, E., Tsichritzis, T., Farmer, H., Ashworth, A., and Mosialos, G. (2003) *Nature* **424,** 793–796

Transient IκB Kinase Activity Mediates Temporal NF-κB Dynamics in Response to a Wide Range of Tumor Necrosis Factor- α Doses

Raymond Cheong, Adriel Bergmann, Shannon L. Werner, Joshua Regal, Alexander Hoffmann and Andre Levchenko

J. Biol. Chem. 2006, 281:2945-2950.
doi: 10.1074/jbc.M510085200 originally published online December 1, 2005